# Motion and heat transfer in the Blasius flow containing a pulsating component

**Heung Weon Cho and Jae Min Hyun**
Department of Mechanical Engineering, Korea Advanced Institute of Science and Technology, Seoul, Korea

Studies are made of the unsteady flow and heat transfer characteristics in the laminar boundary layer about a flat plate when the oncoming free stream contains a pulsating component. The complete, unsteady, boundary layer equations are solved by using a recently-developed numerical solution procedure. A wide range of the two key external parameters in the free stream, i.e., the amplitude of pulsation, $A$, and the frequency parameter $\alpha$ [$\equiv \omega x^*/U_e$], is dealt with in the present numerical computations. Comprehensive and systematically organized numerical computational results have been acquired, providing descriptions of the details of unsteady flow and thermal fields. The present numerical results indicate consistency with the available data based on the previous linearized analytical predictions in the limits of $\alpha \ll 1$ and $\alpha \gg 1$. When the frequency parameter $\alpha$ is small, the flow in the entire depth of the boundary layer exhibits a phase lead over the oncoming free stream. The present computational results supply the details of the behavior of flow and skin friction in the range of intermediate values of $\alpha$ and for finite values of $A$. The thermal structure is scrutinized by using the computed results. The mean temperature field is found to be substantially unaffected by the presence of the pulsating component. For small values of $\alpha$, both the skin friction and heat transfer are in phase with each other. However, as $\alpha$ increases, the conventional Reynolds analogy is shown to be inapplicable.

**Keywords:** Blasius flow; pulsating component; skin friction and heat transfer at the plate

## Introduction

Considerable interest has recently been shown on the general characteristics of unsteady viscous flows about a body (see, e.g., Telionis[1]). Attempts to predict the flow by analytical means have encountered formidable difficulties due to the inherent complexities stemming from the basic flow unsteadiness; and the lack of comprehensive and validated experimental measurements data has been a major obstacle for a rapid progress in research in this area. However, it is now obvious that an improved understanding of unsteady phenomena is essential to develop high-performance fluid machinery, aircraft, and rotorcraft, to name a few.

Most of the prior work has dealt with the cases of two-dimensional external flow about a fixed body, when the oncoming free stream contains a time-dependent part. The bulk of the previous investigations treated unsteady, incompressible, two-dimensional boundary layer flows, and only a few cases considered the attendant heat transfer (Lighthill,[2] Pedley,[3] Ackerberg and Phillips,[4] etc.). Because of the limited computing capabilities in the past, these studies were largely theoretical in nature, and the analyses were restricted to greatly simplified situations for the ease of mathematical tractability. This also implies that critical assessments of these simplified predictions have not been checked against other reliable results based on more elaborate computational schemes.

One of the canonical flow configurations is the motion past a semi-finite flat plate when the oncoming free stream velocity $U_e$ contains a pulsating component, i.e.,

$$U_e = U_m(1 + A \cos \omega t^*) \tag{1}$$

where $\omega$ is the pulsation frequency, $t^*$ is the dimensional time and $A$ is the amplitude of pulsation. Also, the plate is maintained at constant temperature $T_w$ and the free stream temperature at $T_\infty$. The fluid motion described above is essentially the well-known Blasius flow with a time-dependent harmonic oscillation superimposed. The geometrical simplicity of the flow configuration affords a rich testing ground for analytical manipulations; consequently, we can concentrate on the flow and heat transfer structures affected by the unsteadiness, without having to be embroiled with the complicated auxiliary features. In addition, this simple flow provides a host of practical applications in realistic industrial environments; such unsteady fluctuations superimposed on the Blasius flow are of frequent occurrence in fluid machinery, and in the laboratory they can be relatively easily realized by acoustic means.

For the classic model problem flow of Equation 1, Lighthill[2] presented an extensive theoretical exposition for the cases when the fluctuating amplitude $A$ is small. This led to a linearization of the problem formulation. The results of his elaborate analytical investigations disclosed that the maxima of skin friction at any point anticipated the maxima of the stream velocity. He also revealed that different flow regimes could be observed depending on whether the pulsating frequency $\omega$ was greater or smaller than the critical frequency $\omega_c$. Lighthill proceeded to predict that the maxima in heat transfer lagged behind those of the stream velocity. In summary, the principal findings that had emerged out of the pioneering analyses of Lighthill set the stage for the subsequent analytical attempts for a class of unsteady boundary layer flows.[5] Following the analytical methodologies expounded by Lighthill,[2] Ackerberg and Phillips[4] conducted asymptotic and numerical analyses of

Address reprint requests to Dr. Hyun at the Department of Mechanical Engineering, Korea Advanced Institute of Science and Technology, P.O. Box 150, Chong Ryang, Seoul, Korea.

Received 27 February 1989; accepted 15 May 1989

© 1989 Butterworth Publishers

## Notation

| | |
|---|---|
| $A$ | Amplitude of fluctuation in the free stream |
| $Cf$ | Skin friction coefficient |
| $L$ | Characteristic stream-wise length scale |
| Nu | Nusselt number at the wall |
| $Pr$ | Prandtl number, $\nu/\kappa$ |
| $q$ | Heat flux |
| $R_L$ | Reference Reynolds number, $U_m L/\nu$ |
| $St$ | Stanton number, $q_w/\rho_e C_p(T_w - T_\infty)U_m$ |
| $T^*$ | Dimensional temperature |
| $t, t^*$ | Nondimensional, dimensional time |
| $U_e$ | Oncoming free-stream velocity |
| $u, v$ | Nondimensional velocity components |
| $u^*, v^*$ | Dimensional velocity components |
| $x, y$ | Nondimensional coordinates |
| $x^*, y^*$ | Dimensional coordinates |
| $\alpha$ | Nondimensional frequency parameter, $\omega x^*/U_m$ |
| $\theta$ | Nondimensional temperature |
| $\phi_u, \phi_C, \phi_\theta, \phi_N$ | Phase angles |
| $\kappa$ | Thermal diffusivity |
| $\nu$ | Kinematic viscosity |
| $\omega, \omega_c$ | Pulsation frequency, critical frequency |

the linearized ($A \ll 1$) unsteady boundary layer equations. They obtained asymptotic solutions in the limits $\alpha\ [\equiv \omega x^*/U_m] \to 0$ and $\alpha \to \infty$, where $x^*$ denotes the coordinate in the plane of the flat plate from the leading edge. Using generally similar mathematical approaches, Pedley[3] extended the analyses to the cases when the restriction $A \ll 1$ was relaxed. He demonstrated that two expansion schemes were obtainable for the limiting cases of small and large values of $\alpha$. It was shown feasible that an overlapping region between the above two limits could be mapped out by constructing a suitable mathematical asymptotic representation.

The previous work cited above has substantially deepened our knowledge on the overall dynamic characteristics germane to the unsteady boundary layer exemplified by Equation 1. However, these studies were highly theoretical and limited in scope. A number of simplifying assumptions had to be invoked during the course of analysis.

A review of the above mathematical treatises clearly suggests that independent and more thorough investigations of the flow posed in Equation 1 by other means would be of great usefulness. The outcome of such studies will be valuable to cross-check the predictions of the above highly simplified theoretical accounts and enable us to describe the flow structure over a broad range of the parameter values. On the experimental side, as observed by Kwon, Pletcher, and Delaney,[6] accurate data based on laboratory measurements are scarce in the literature. As to the flow described by Equation 1, Hill and Stenning[7] presented rudimentary experimental data of the flow structure which were obtained by using a simple open-circuit suction type wind tunnel.

One remaining promising approach is obtaining direct numerical solutions to the appropriate boundary layer equations. Owing to the extreme complexities involved in computing the unsteady flows over a broad range of external conditions, constructing a widely applicable and versatile numerical algorithm is a formidable undertaking. However, the recent progress in computational capabilities has facilitated the advent of a reliable numerical solution procedure to calculate the unsteady boundary layer flows on a simple geometry. Among others, in a series of publications, Kwon *et al.*[6,8] presented a new and powerful numerical methodology to tackle the general unsteady, two-dimensional boundary layer flows. This solution procedure utilized the primitive variables and used an extension of the fully implicit numerical algorithm.[6] They devised a numerical model applicable to both laminar and turbulent boundary layers. In an effort to verify the accuracy and capabilities of their numerical model, they made several sample calculations of well-established simple unsteady flows. The computed results exhibited generally satisfactory agreement with the available measured data and/or analytical solutions for the sample flows. These favorable comparisons have clearly demonstrated the usefulness and effectiveness of the numerical solution procedure of Kwon *et al.*[6,8] to examine a variety of unsteady boundary layer flows.

The purpose of the present study is to carry out a comprehensive and in-depth examination of the laminar unsteady flow given by Equation 1 by numerically integrating the complete nonlinear time-dependent boundary layer equations. Since the fully numerical approaches are exploited, no restrictions, in principle, on the magnitude of $A$ (except that $0 < A < 1$) or $\omega$ will be made. One of the primary objectives is to depict the full details of the time-averaged velocity and temperature structures over wide ranges of the frequency $\omega$ and the amplitude of pulsation $A$. This information will provide a valuable check to validate the theoretical predictions which were obtained under several restrictive assumptions, i.e., $A \ll 1$, $\alpha \ll 1$ and $\alpha \gg 1$, etc. Of special interest is the description of the unsteady behavior of the skin friction and the heat transfer on the plate, both in terms of the amplitude variations and the phase differences. We will be particularly concerned with the flow and heat transfer characteristics when the frequency parameter $\alpha\ [\equiv \omega x^*/U_m]$ takes moderate values in between the limits $\alpha \ll 1$ and $\alpha \gg 1$. This has not been dealt with by the earlier analytical investigations, and it is important to illustrate the flow structures covering the entire range of the frequency values. By resorting to full-scale numerical calculations, we intend to fill the gap with the precise flow data linking the two extreme cases of small and large $\alpha$. In the present study, emphasis will also be placed on the effect of finite values of $A$ on the overall flow and heat transfer characteristics. This capability is significant in that the previous analytical methodology had been constrained by the requirement $A \ll 1$.

The numerical solution techniques adopted in the present paper follow closely those given by Kwon *et al.*[6] The principal dynamic features peculiar to the unsteady boundary layer flows about a flat plate will be clearly identified and discussed. The numerical results of this paper will furnish useful source materials on the flow details; the results of future endeavors, numerical or experimental, can be compared against this information to assist in checking the consistency of their data.

## The problem formulation

We introduce the two-dimensional Cartesian coordinates, with the semi-infinite flat plate coinciding with the $x$ axis, and the $y$ axis perpendicular to the plate at the leading edge. The complete unsteady, incompressible laminar boundary layer equations, in properly nondimensionalized form, are well

known (e.g., Schlichting[9]).

$$\frac{\partial u}{\partial x}+\frac{\partial u}{\partial y}=0 \tag{2}$$

$$\frac{\partial u}{\partial t}+u\frac{\partial u}{\partial x}+v\frac{\partial u}{\partial y}=\frac{\partial U_e}{\partial t}+\frac{\partial^2 u}{\partial y^2} \tag{3}$$

$$\frac{\partial \theta}{\partial t}+u\frac{\partial \theta}{\partial x}+v\frac{\partial \theta}{\partial y}=\frac{1}{Pr}\frac{\partial^2 \theta}{\partial y^2} \tag{4}$$

In the above, $u$ and $v$ are the velocity components in the $x$ and $y$ directions; $U_e$ denotes the free stream velocity at the boundary layer edge condition, expressed in Equation 1; $\theta$ the temperature; $Pr$ the Prandtl number ($Pr=\nu/\kappa$, $\nu$ the kinematic viscosity, and $\kappa$ the thermal diffusivity). In the present problem formulation for an incompressible flow, the viscous dissipation has been neglected and all the physical properties are taken to be constant.

In view of the imposed unsteady free stream velocity, the nondimensionalization has naturally been based on using the following reference values for the respective dimensional physical quantities (starred)

$$u\equiv u^*/U_m, \qquad x\equiv x^*/L, \qquad t\equiv t^*/(L/U_m)$$

$$v\equiv v^*/(RL^{-1/2}\cdot U_m), \qquad y\equiv y^*/(RL^{-1/2}\cdot L)$$

where $RL\equiv U_m L/\nu$ and the nondimensional temperature $\theta=(T^*-T_\infty)/(T_w-T_\infty)$, where $T^*$ denotes the dimensional temperature and $T_\infty$ and $T_w$ the temperatures of the free stream and of the wall, respectively. The characteristic streamwise length scale $L$ is chosen such that $L$ defines the extent of the computational domain in the streamwise direction.[6,8]

The associated boundary conditions are

$$\text{at } y=0, \qquad u(x,0,t)=0 \tag{5a}$$

$$v(x,0,t)=0 \tag{5b}$$

$$\theta(x,0,t)=1 \tag{5c}$$

$$\text{as } y\to\infty, \qquad u(x,y,t)\to 1+A\cos \alpha t/x \tag{5d}$$

$$\theta(x,y,t)\to 0 \tag{5e}$$

Note that the velocity boundary condition at the edge of the boundary layer, Equation 5d is derived as a result of the above-stated nondimensionalizations adopted in the present paper. As is clear in Equation 5d, the effects of the pulsating free stream are characterized by the two nondimensional quantities, i.e., $A$, the amplitude of pulsation, and the frequency parameter $\alpha=\omega x^*/U_m$.

The significance of the dimensionless frequency parameter $\alpha$ was brought into focus by the earlier theoretical analyses.[3,4] It was shown that $\alpha$ was used as the key expansion parameter such that the property of the solution in the limiting cases of $\alpha\to 0$ and $\alpha\to\infty$ could be determined. In the present problem formulation, therefore, there exists a certain degree of equivalence of small $x^*$ with small $\omega$ and large $x^*$ with large $\omega$.[4] It is also important to recognize that, due to the nondimensionalization schemes, the pulsating component is expressed by a combination of $x$ and $t$, as shown in Equation 5d.

The main task is to find a suitable numerical solution technique for the system of partial differential equations 2–5; the technique should be flexible enough to be applicable over a wide range of the externally specifiable parameters $A$ and $\alpha$.

## Numerical method

The numerical solution schemes that were adopted in the present paper are essentially based on those documented by Kwon *et al.*[6] Full details, including the finite-difference representations of all the terms in Equations 2–5, were succinctly described by Kwon *et al.* (see equations 13–16 of Ref. 6). The readers are referred to the above-cited papers for the highlights of the numerical model development.

The finite-difference equations were solved effectively by the block-elimination method discussed by Cebeci and Bradshaw[10] and Bradshaw.[11] This methodology calls for local iterations to obtain the solutions that satisfy the governing equations simultaneously at each streamwise station. In the present numerical computations, typically 4–5 iterations were required for the local iteration to achieve the convergence criterion, i.e., the variations of streamwise velocity gradient at the wall between two successive iterations should be less than a prescribed accuracy level ($10^{-6}$ in the present study). At the initial instant, the well-known steady solution was used as the initial state conditions. Usually, the temporarily periodic solution was attained after 4–6 cycles of pulsating oscillations. The time resolution of the solutions was such that 80 time steps constituted one pulsating cycle. The spatial mesh used was typically $101\times 51$ in the $x$-$y$ computational domain.

## Results and discussion

As mentioned previously, the unsteady flow conditions that are externally specifiable are $A$ and $\alpha$ in Equation 5d. In an effort to produce comprehensive and systematic results in broad ranges of parameters, values of the frequency parameter $\alpha$ up to 15.0 were selected for computations. The Prandtl number was set $Pr=0.72$ to model air. Three different values of the amplitude factor $A$, $A=0.01$, 0.10 and 0.20, were used in the calculations. These values were chosen in order to validate the earlier linearized theoretical predictions (i.e., by using $A=0.1$), and to explore the nonlinear regimes as the pulsating amplitude $A$ increases accordingly. It should be remarked that, in view of the nature of the oncoming free stream, significant flow reversals are possible, especially near the plate, when $A$ increases to an appreciable value. In fact, for the actual computations, considerable numerical difficulties were encountered in obtaining converged solutions when $A$ exceeded about 0.5. These practical considerations preclude the cases when $A$ takes values close to the top end of the range $0<A<1$.

The major computed results on the flow and heat trasfer structures will be displayed by plotting the amplitude and phase angle of the physical quantity of interest relative to the oncoming free stream oscillation. This method was utilized previously by Cebeci.[12]

## The velocity field

One principal physical variable of interest is the velocity component in the streamwise direction, $u$. We now express $u$ as

$$u=u_m+Au_1\cos(\alpha t/x+\phi_u),$$

in which $u_m$ denotes the time-averaged distribution, $u_1$ the normalized amplitude of the pulsating part, and $\phi_u$ the phase angle relative to the free stream oscillation.

Figure 1 exemplifies the profile of $u_m$. It is evident that the averaged velocity profile remains virtually unaffected by the presence of the pulsating part in the free stream. Figure 1 serves the additional purpose to give credence to the accuracy and reliability of the present numerical solutions. As pointed out by Kwon *et al.*,[6] the structure of $u_m$ is largely similar to that of the standard steady-state Blasius solution, and Figure 1 bears out this point. It is also important to observe that, for the entire

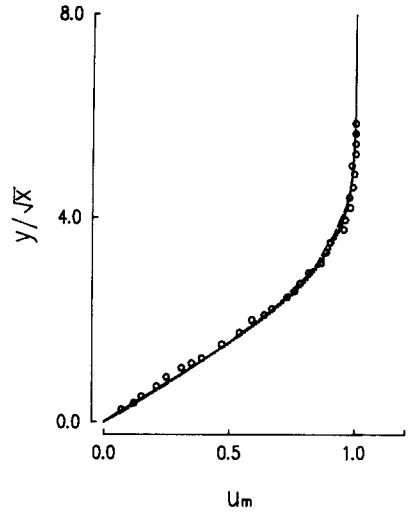


*Figure 1* Exemplary profile of the mean streamwise velocity, $u_m$. ——, the present calculations; · · · · ·, the standard Blasius solution; – – –, calculations of Ref. 6; ○, measurement data of Ref. 7

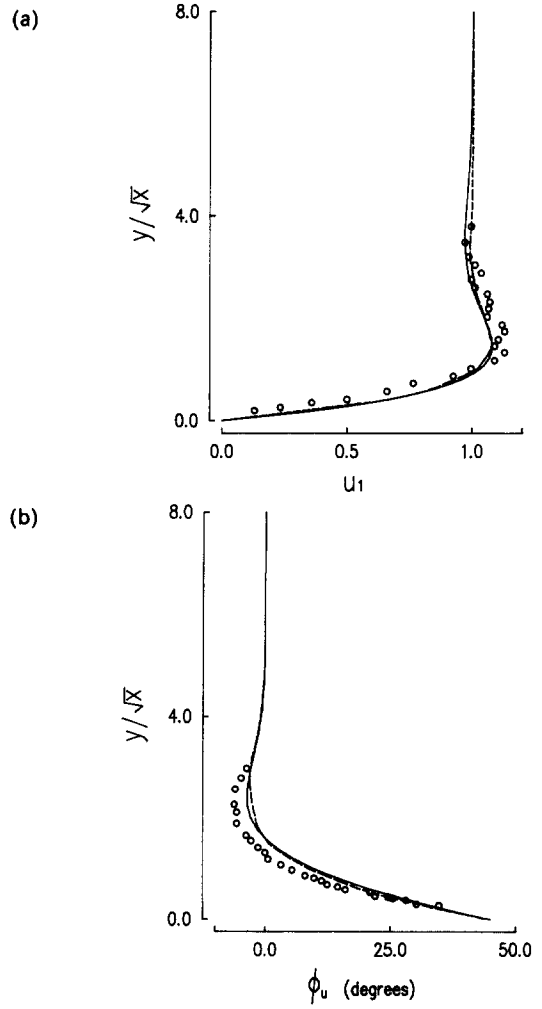


*Figure 2* (a) Amplitude of the fluctuating part of the streamwise velocity, $u_1$ for large values of $\alpha$. ——, the present calculations, $A=0.1$, $\alpha=4.72$; – – –, calculations of Ref. 14, $A=0.1$, $\alpha=4.98$; ○, data of Ref. 7, $A=0.09$, $\alpha=4.98$. (b) Phase of the fluctuating part of the streamwise velocity, $\phi_u$, for large values of $\alpha$. ——, the present calculations, $A=0.1$, $\alpha=4.72$; – – –, calculations of Ref. 14, $A=0.1$, $\alpha=4.98$; ○, data of Ref. 7, $A=0.09$, $\alpha=4.98$

set of the runs computed, the $u_m$ profile is substantially independent of $A$ and $\alpha$.

In order to further verify the present numerical results, computations were performed using the parameter values similar to those available in the published experimental data.[7] The amplitude of the pulsating part $u_1$ and the phase angle $\phi_u$ are depicted in Figures 2(a), 2(b) and 3(a), 3(b), each of which is representative of the flow pattern for a high frequency and a low frequency oscillation, respectively. As demonstrated in these figures, the computed results are found to be consistently in broad agreement with the available data obtained by other means.[12,13,14] In particular, in the high frequency regime, the present results satisfactorily reproduce the maximum oscillation amplitude and minimum phase angle, which are the characteristic features of a pulsating Blasius flow. The published data in the literature are rather limited, but the comparisons illustrated here establish the capability and correctness of the present numerical solutions over a wide range of the parameter space.

We shall now turn to the depiction of the complete flow

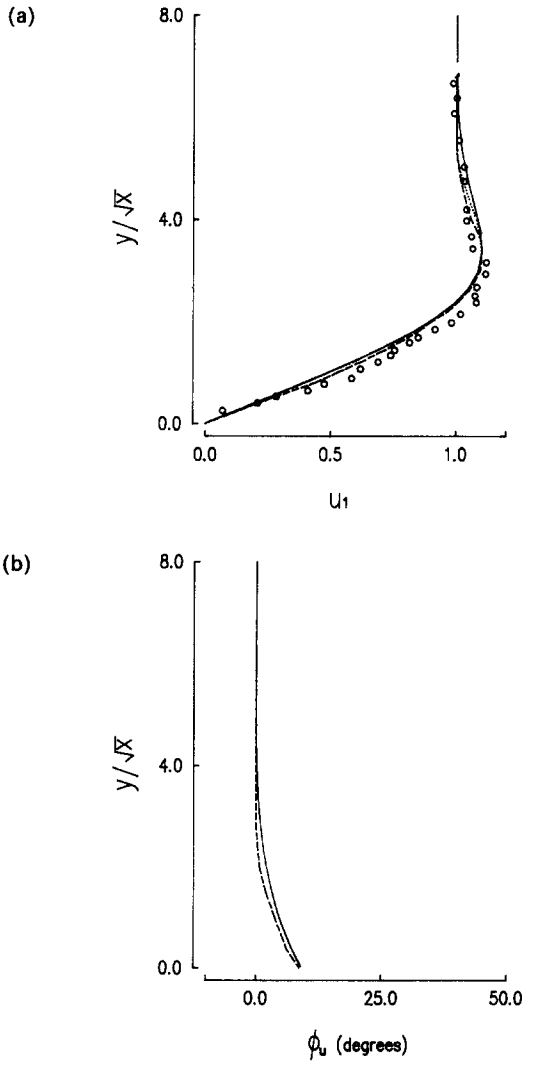


*Figure 3* (a) Amplitude of the fluctuating part of the streamwise velocity, $u_1$, for small values of $\alpha$. ——, the present calculations, $A=0.1$, $\alpha=0.094$; · · · · ·, calculations of Ref. 14, $A=0.1$, $\alpha=0.103$; – – –, calculations of Ref. 13, $A=0.15$, $\alpha=0.103$; ○, data of Ref. 7, $A=0.15$, $\alpha=0.103$. (b) Phase of the fluctuating part of the streamwise velocity, $\phi_u$, for small values of $\alpha$. ——, the present calculations, $A=0.1$, $\alpha=0.094$; – – –, calculations of Ref. 14, $A=0.1$, $\alpha=0.103$

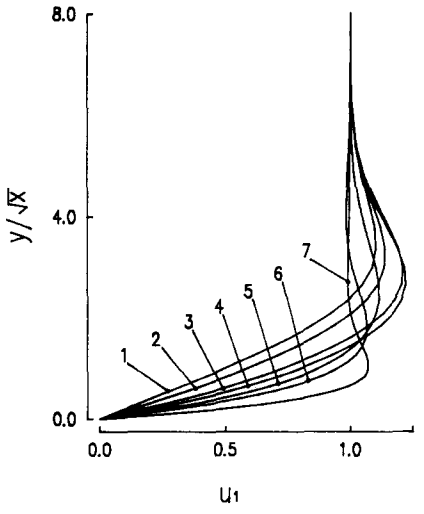


*Figure 4* Profiles of $u_1$. Curve 1, $\alpha=0.09$; 2, $\alpha=0.47$; 3, $\alpha=0.94$; 4, $\alpha=1.41$; 5, $\alpha=2.36$; 6, $\alpha=3.30$; 7, $\alpha=9.43$. The values of $A$ for this run is 0.1, however, the behavior of $u_1$ is found to be insensitive to the variations of $A$

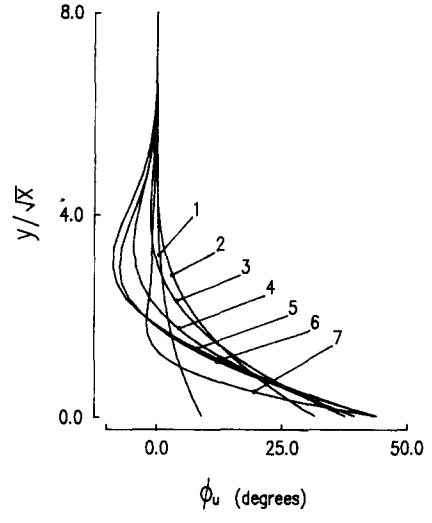


*Figure 5* Profiles of $\phi_1$. Curve 1, $\alpha=0.09$; 2, $\alpha=0.47$; 3, $\alpha=0.94$; 4, $\alpha=1.41$; 5, $\alpha=2.36$; 6, $\alpha=3.30$; 7, $\alpha=9.43$. The values of $A$ for this run is 0.1, however, the behavior of $\phi_u$ is found to be insensitive to the variations of $A$

details afforded by the present numerical computations. Figures 4 and 5 exhibit the results of an extensive parametric study delineating the behavior of the pulsating part of the flow over a wide range of $\alpha$ for $A=0.1$. The computed results are found to be insensitive to the variation of $A$; Figures 4 and 5 exemplify the overall trend of the oscillatory velocity component.

For low values of $\alpha$, the influence of the imposed free stream oscillation is comparatively minor in the region close to the plate. The magnitude of the oscillatory part of the velocity increases with $y$. The oscillation amplitude reaches a maximum at a moderate value of $y$, and for $y$ beyond this maximum point, the oscillation amplitude monotonically decreases toward the value of the oncoming free stream oscillation. The phase angles are entirely positive for these situations, indicating that a phase lead takes place for the velocity field in the whole region of the boundary layer. The phase lead decreases with increasing $y$, and as expected, it decays to zero near the edge of the boundary layer.

As $\alpha$ increases, the maximum amplitude increases until $\alpha$ reaches a critical value of approximately 1.5. As $\alpha$ increases further beyond this value, the maximum amplitude is somewhat smaller, and the $y$ location for maximum $u_1$, $y_{max}$, moves rather close to the plate. At large values of $\alpha$, the phase lead at the plate tends to converge to a value of 45 degrees, but a phase lag exists in the outer portion of the boundary layer. As is intuitively clear, at very large values of $\alpha$, the bulk of the boundary layer oscillates in tune with the imposed free stream oscillation, i.e., $u_1 \to 1$, $\phi_u \to 0$, except in a narrow strip adjacent to the solid plate. Physically speaking, the fluid in the near vicinity of the plate oscillates with a $\pi/4$-rad phase lead relative to the free stream oscillation, but the influence of the plate quickly diminishes as $y$ increases.

As to the phase difference of the velocity field, Lighthill[2] proposed plausible explanations based on an insightful physical reasoning. He argued that the additional pressure gradient required to accelerate the main stream was responsible for the phase lead, and the phase lag was caused by the inertia of the fluid resisting the quasi-steady fluctuations. In the inner portion of the boundary layer close to the plate, the former effect is dominant, thus a phase lead results; on the other hand, in the outer portion of the layer, the latter effect slightly outweighs the former, which produces a small phase lag. The computed velocity field shown in Figures 1–5 is supportive of the principal contentions of the theoretical expositions cited above.

A physical quantity of great interest in engineering applications is the wall shear stress, $Cf$. In a manner similar to the previous developments,[4,12,15] $Cf$ is written as a sum of the time-averaged part and the oscillating part, i.e.,

$$Cf = Cf_m\left[1 + A\frac{Cf_1}{Cf_m}\cos(\alpha t/x + \phi_C)\right]$$

Figures 6(a)–(c) display the variations of $Cf_m$, $Cf_1$, and $\phi_C$ as functions of $\alpha$. As is discernible in Figure 6(a), when the amplitude of the free stream pulsation, $A$, is small, $Cf_m$ is virtually indistinguishable from the value for the standard Blasius solution over the entire range of $\alpha$. However, as $A$ increases, the dependence of $Cf_m$ on $\alpha$ becomes apparent. In general, the maximum of $Cf_m$ is achieved at very low frequencies, and the minimum of $Cf_m$ is seen at moderate values of $\alpha$. No published data by other means of investigations on the behavior of $Cf_m$ are available in the literature. Figure 6(b) illustrates the magnitude of the oscillating part of the skin friction. The computational results have been over-plotted to demonstrate the satisfactory agreement with the other calculated data.[10,15] It is evident that the oscillatory part contained in the skin friction increases almost linearly with $\alpha$. The present calculations also indicate that this behavior is virtually independent of $A$. The variation of $\phi_C$ is plotted in Figure 6(c), exhibiting close agreement with the other available computational results. As anticipated, $\phi_C$ increases rapidly with $\alpha$ in the low-frequency region, say, $\alpha<0.7$; however, $\phi_C$ approaches rather slowly the limiting value of 45 degrees as $\alpha$ increases beyond 0.7. The general behavior of $Cf$ shown in Figure 6 is qualitatively consistent with the earlier theoretical solutions in the limiting cases of small and large values of $\alpha$.

## Temperature field

We now shift our attention to the question of heat transfer from the plate to the fluid. Only a few authors have addressed the issue of heat transfer in an unsteady boundary layer. The published data on heat transfer are scanty; we note with interest that Pedley[3] presented a highly mathematical account to determine the heat transfer rate in two extreme circumstances, i.e., when $\alpha \to 0$ and $\alpha \to \infty$. The numerical approach taken in the present study has the advantage that the precise information

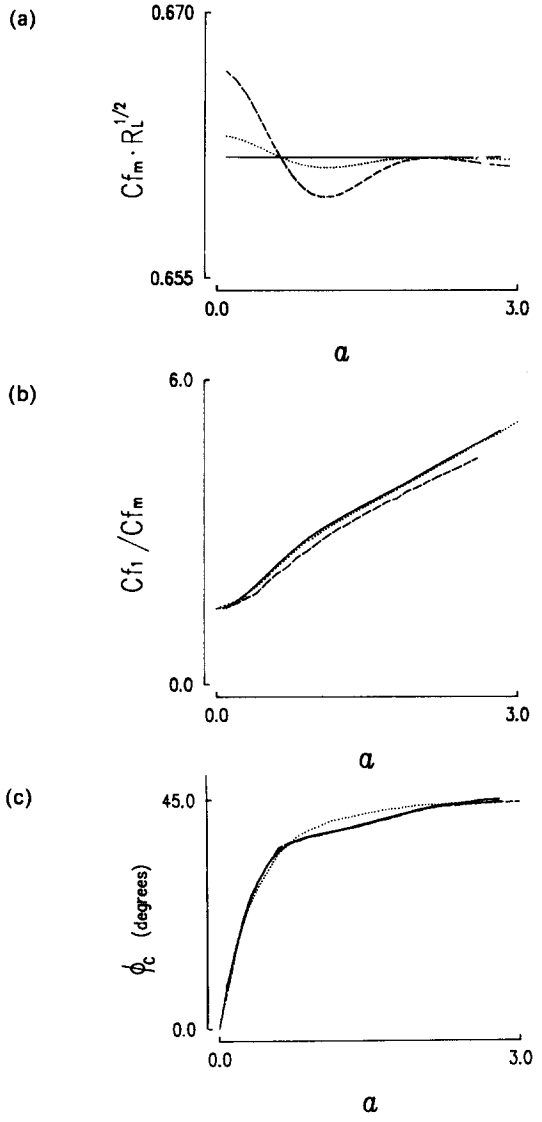


*Figure 6* (a) Variation of the mean skin friction, $Cf_m$, with $\alpha$ at $x=1.0$. ——, $A=0.01$; · · · · ·, $A=0.1$; – – –, $A=0.2$. (b) Variation of the oscillating amplitude of skin friction, $Cf_1/Cf_m$, with $\alpha$. ——, the present calculations; · · · · ·, calculations of Ref. 12; – – –, calculations of Ref. 15. (c) Variations of the phase of the oscillating part of skin friction, $\phi_c$, with $\alpha$. ——, the present calculations; · · · · ·, calculations of Ref. 15; – – –, calculations of Ref. 12; – · – · –, predictions of Ref. 4

on the thermal field is obtainable simultaneously with the flow field data. The temperature $\theta$ and the Nusselt number Nu are decomposed into a time-averaged quantity and an oscillating part;

$$\theta = \theta_m + A\theta_1 \cos(\alpha t/x - \phi_\theta)$$

$$\mathrm{Nu} = \mathrm{Nu}_m \left[ 1 + A \frac{\mathrm{Nu}_1}{\mathrm{Nu}_m} \cos(\alpha t/x - \phi_N) \right]$$

The temperature structure is illustrated in Figures 7, 8, and 9. As shown in Figure 7, the time-averaged temperature profile $\theta_m$ is substantially unaffected by the free stream oscillations, maintaining a profile almost indistinguishable from the steady-state similarity solution. The oscillatory part of the temperature field, $\theta_1$, displays the characteristic feature that the maximum of $\theta_1$ occurs in the mid-depth region of the boundary layer. The magnitude of the maximum of $\theta_1$ is largest when $\alpha$ takes

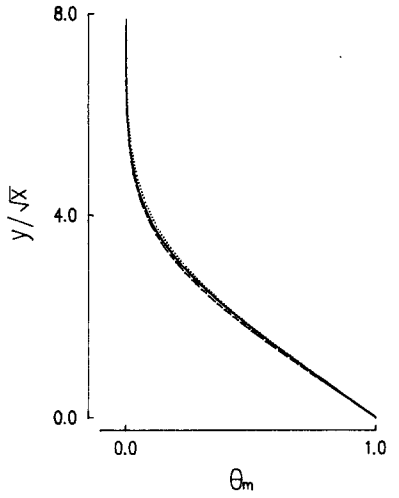


*Figure 7* Exemplary profile of the computed mean temperature, $\theta_m$. ——, the similarity solution; – – –, $A=0.1$; · · · · ·, $A=0.2$

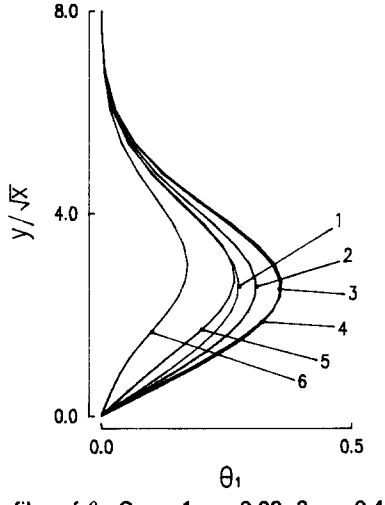


*Figure 8* Profiles of $\theta_1$. Curve 1, $\alpha=0.09$; 2, $\alpha=0.47$; 3, $\alpha=0.94$; 4, $\alpha=1.41$; 5, $\alpha=2.36$; 6, $\alpha=3.11$. The values of $A$ for this run is 0.1, however, the behavior of $\theta_1$ is found to be insensitive to the variations of $A$

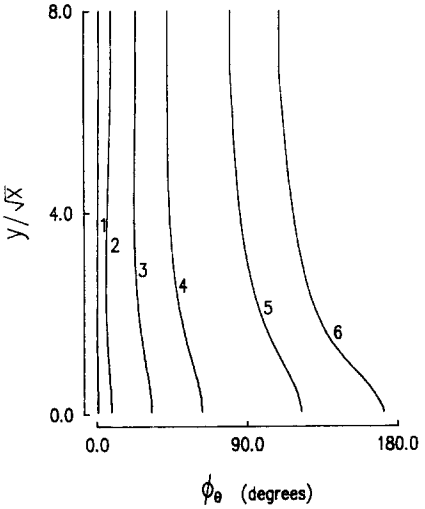


*Figure 9* Profiles of $\phi_\theta$. Curve 1, $\alpha=0.09$; 2, $\alpha=0.47$; 3, $\alpha=0.94$; 4, $\alpha=1.41$; 5, $\alpha=2.36$; 6, $\alpha=3.11$. The values of $A$ for this run is 0.1, however, the behavior of $\phi_\theta$ is found to be insensitive to the variations of $A$

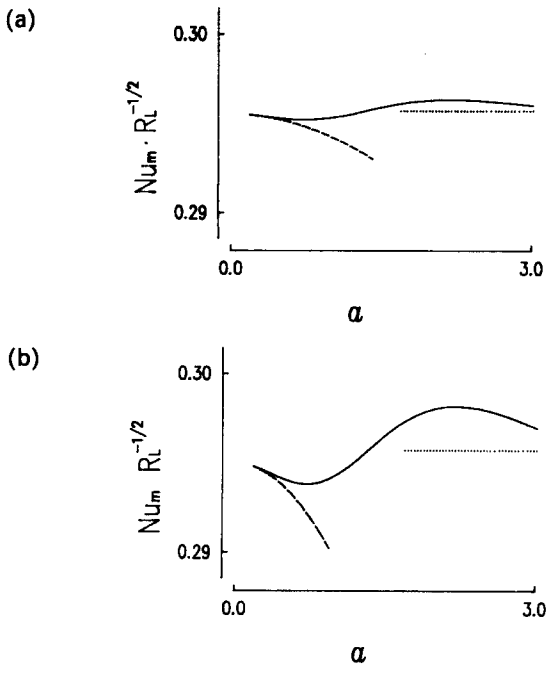


*Figure 10* (a) Variations of the mean Nusselt number, $Nu_m$, with $\alpha$ for $A=0.1$ at $x=1.0$. ——, the present calculations; · · · · ·, predictions of Ref. 3 for the high-$\alpha$ limit; – – –, predictions of Ref. 3 for the low-$\alpha$ limit. (b) Variations of the mean Nusselt number, $Nu_m$, with $\alpha$ for $A=0.2$ at $x=1.0$. ——, the present calculations; · · · · ·, predictions of Ref. 3 for the high-$\alpha$ limit; – – –, predictions of Ref. 3 for the low-$\alpha$ limit

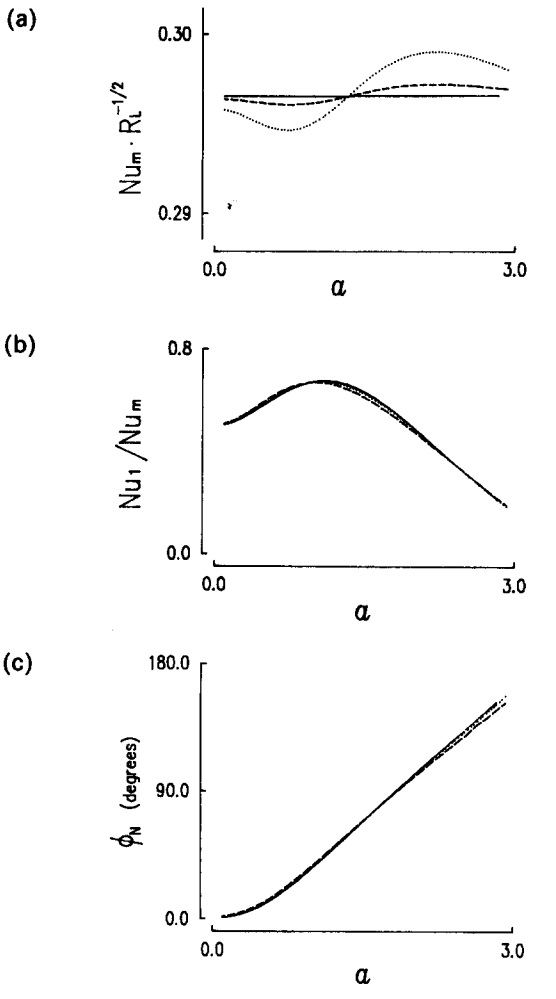


*Figure 11* (a) Variation of the mean Nusselt number, $Nu_m$, with $\alpha$ at $x=1.0$. ——, $A=0.01$; – – –, $A=0.1$; · · · · ·, $A=0.2$. (b) Variation of the oscillatory amplitude of Nusselt number, $Nu_1/Nu_m$, with $\alpha$. ——, $A=0.01$; · · · · ·, $A=0.1$; – – –, $A=0.2$. (c) Variation of the phase of the oscillating part of Nusselt number, $\phi_N$, with $\alpha$. ——, $A=0.01$; · · · · ·, $A=0.1$; – – –, $A=0.2$

a moderate value, around $\alpha \cong 1.2$. The phase of the temperature field generally increases mildly as $y$ approaches the wall.

Figures 10(a),(b) plot the variation of $Nu_m$ versus $\alpha$, together with the analytical solutions of Pedley[3] in the two limits. The present numerical results are clearly corroborative of the theoretical predictions of Pedley. The analytical formalism of Pedley apparently fails to produce a viable solution in the overlapping region linking the two extreme limiting solutions, and the difficulty with Pedley's solutions appears to become more pronounced as $A$ increases. The behavior of the oscillatory part in heat transfer is shown in Figures 11(b),(c). The profiles of $Nu_1$, and $\phi_N$ are insensitive to the magnitude of $A$. Inspection of Figures 6 and 11 reveals that the phase of heat transfer differs from that of the skin friction.

In order to ascertain the relationship in the phases of skin friction and heat transfer, Figure 12 shows the computed periodic solutions of wall shear stress and Stanton number, $St$ $[\equiv q_w/\rho_e C_p(T_w - T_\infty)U_e]$, at the same streamwise location. As is clearly discernible in Figure 12, for small values of $\alpha$, both the skin friction and heat transfer execute the periodic cycle in tune with each other. However, for moderate and large values of $\alpha$, the character of these two shows considerable discrepancies. As $\alpha$ increases, the skin friction coefficient increases in magnitude and advances slightly in phase, but the heat transfer displays a generally opposite trend. Notice that, as shown in Figure 12(d) for $\alpha=3.1$, the phase difference between the two attains 180 degrees. This clearly points to the conclusion that the quasi-steady Reynolds analogy holds good only for very small values of $\alpha$; the often-cited Reynolds analogy loses its validity as the value of $\alpha$ becomes appreciable. This finding, based on detailed and explicit numerical examinations of the present study, gives strong support to the observations made by Lighthill[2] and Kwon *et al.*[6]

## Conclusions

Comprehensive and systematic numerical calculations have been made of the unsteady boundary layer equations about a Blasius flow with a periodic fluctuating component. The numerical computations were conducted to acquire accurate details of the flow and thermal structures over wide ranges of the parameter values.

The profiles of the mean streamwise velocity are found to be quite similar to the standard Blasius solution. The computed results of the fluctuating parts of the streamwise velocity are consistent with the previous theoretical results in the limits of $\alpha \ll 1$ and $\alpha \gg 1$. For small values of $\alpha$, there is an overall phase lead across most of the boundary layer.

The computational results of the skin friction indicate that the maximum of $Cf_m$ is achieved at very small values of $\alpha$, and the minimum of $Cf_m$ occurs at moderate values of $\alpha$. The general behavior of the fluctuating part of the skin friction exhibits consistency with the theoretical solutions in the limiting cases.

The details of the thermal structure are examined by using the computational results. The field of the mean temperature is substantially unaffected by the presence of the pulsating

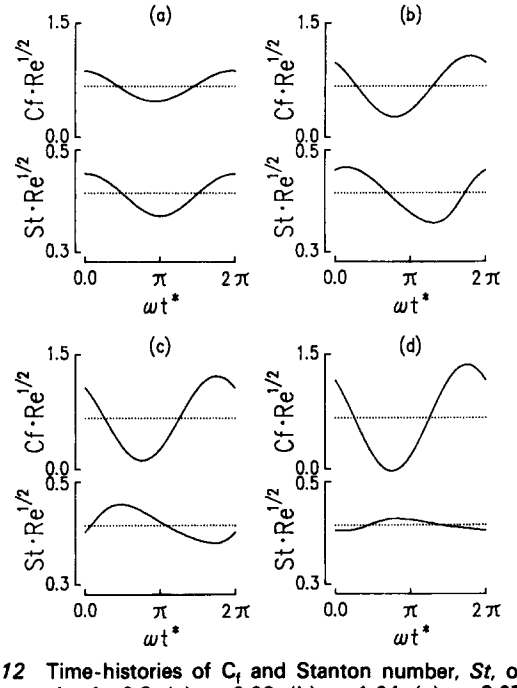


*Figure 12* Time-histories of $C_f$ and Stanton number, *St*, over a pulsating cycle. $A=0.2$, (a) $\alpha=0.09$; (b) $\alpha=1.04$; (c) $\alpha=2.07$; (d) $\alpha=3.11$

component. The amplitude of the fluctuating part is largest when $\alpha$ takes moderate values.

For small values of $\alpha$, both the skin friction and heat transfer execute the periodic cycle in tune with each other. However, as $\alpha$ increases, the conventional Reynolds analogy, which is applicable when $\alpha$ is small, loses its validity.

## References


1 Telionis, D. P. Review—Unsteady boundary layers, separated and attached. *ASME J. Fluids Engng.*, 1979, **101**, 29–43

2 Lighthill, M. J. The response of laminar skin friction and heat transfer to fluctuations in the stream velocity. *Proc. Roy. Soc.*, 1954, **224A**, 1–23

3 Pedley, T. J. Two-dimensional boundary layers in a free stream which oscillates without reversing. *J. Fluid Mech.*, 1972, **55**, 359–383

4 Ackerberg, R. C. and Phillips, J. H. The unsteady laminar boundary layer on a semi-infinite flat plate due to small fluctuations in the magnitude of the free-stream velocity. *J. Fluid Mech.*, 1972, **51**, 137–157

5 Rosenhead, L. *Laminar Boundary Layers.* Oxford University Press, Oxford, 1963

6 Kwon, O. K., Pletcher, R. H., and Delaney, R. A. Solution procedure for unsteady two-dimensional boundary layers. *ASME J. Fluids Engng.*, 1988, **110**, 69–75

7 Hill, P. G. and Stenning, A. H. Laminar boundary layers in oscillatory flow. *ASME J. Basic Engng.*, 1960, 593–608

8 Kwon, O. K. Calculation of unsteady turbulent boundary layers. ASME paper, 1987, 87-GT-53, 1–8

9 Schlichting, H. *Boundary-Layer Theory.* 7th ed., McGraw-Hill, 1979

10 Cebeci, T. and Bradshaw, P. *Momentum Transfer in Boundary Layers*, McGraw-Hill, 1977

11 Bradshaw, P. *Physical and Computational Aspects of Convective Heat Transfer.* Springer-Verlag, 1984

12 Cebeci, T. Calculation of unsteady two-dimensional laminar and turbulent boundary layers with fluctuations in external velocity. *Proc. Roy. Soc.*, 1977, **355A**, 225–238

13 Orlandi, P. and Ferziger, J. H. Implicit noniterative schemes for unsteady boundary layers. *AIAA J.*, 1981, **19**, 1408–1414

14 Menendez, A. N. and Ramaprian, B. R. Prediction of periodic boundary layers. *Int. J. Num. Meth. in Fluids*, 1984, **4**, 781–800

15 McCroskey, W. J. and Philippe, J. J. Unsteady viscous flow on oscillating airfoils. *AIAA J.*, 1975, **13**, 71–79

# Heat transfer to a continuous moving flat surface with variable wall temperature

**S. T. Revankar**
Department of Nuclear Engineering, Purdue University, West Lafayette, IN, USA

Transient heat transfer from a continuous moving flat surface with varying wall temperature is studied. Numerical results are presented for the transient temperature profiles and heat transfer rates from the wall for Prandtl numbers varying from 0.01 to 1000. Asymptotic solutions for steady state heat transfer rates for large Prandtl number are also presented.

**Keywords:** continuous moving plate; transient and steady-state heat transfer; varying wall temperature

## Introduction

The study of heat transfer or mass transfer to and from a continuous flat surface moving at high speed is of considerable practical interest. Such systems are used in the fabrication of sheet glass, steel plates, paper drying, electrotinning of steel sheets and copper wire, hot rolling, hot extrusion, cold extrusion and continuous casting. Sakiadis[1-3] was the first to study this class of boundary layer problem, where a numerical solution was obtained for two-dimensional flow induced by a long moving plate or cylinder using similarity transformation. Experimental investigations of the flow field were made by Tsou *et al.*[4] and Griffith.[5] Numerical solutions of the steady-state thermal boundary layers on the continuous flat surface have been obtained by Tsou *et al.*,[4] Rhodes and Kaminer,[6] Erickson *et al.*,[7] and by Rotte and Beek,[8] Bourne and Elliston,[9] and Karmis and Pechoc[10] in case of cylindrical surfaces. In these works the thickness of the plate or material was considered to be negligibly small as compared to the distance along the surface. Griffin and Throne[11] have reported an experimental study of heat transfer from a continuously moving belt in air. Their results were in agreement with the theoretical results of Erickson *et al.*[7]

However, in cases such as in continuous casting, the thickness of the emerging plate is finite; hence, one has to consider the conduction within the plate. Karwe and Jaluria[12,13] have included the conjugate transport resulting from conduction within finite size plate while analyzing the heat transport from a continuous moving plate. In case of continuous extrusion of the polymer from a die, the thin polymer sheet or filament constitute a continuous moving solid with a nonuniform surface velocity and temperature.[14] Soundalgekar and Murty[15] used power law surface temperature to investigate steady-state heat transfer from a continuous moving surface. Jeng *et al.*[16] further considered orbitrary surface velocity and nonuniform surface temperature for this problem.

As the analysis of the boundary layer near continuously moving surface is similar for the cases of heat transfer and mass transfer, the results obtained for heat transfer characteristics can be used in case of mass transfer by replacing the Prandtl and Nusselt numbers respectively by Schmidt and Sherwood numbers. Chin[17] presented an asymptotic solution valid for large Schmidt numbers for mass transfer to a continuously moving plate under laminar conditions. Gorla has studied the transient mass transfer to a continuous moving plate with step change in surface concentration[18] and with step change in surface mass flux[19] using similarity transformation. These results can be used for heat transfer case with uniform wall temperature and uniform heat flux condition.

As this problem is of interest to both heat transfer and mass transfer cases, the present note considers transient heat transfer from continuous moving plate with step change in variable wall temperature. The variation in wall temperature considered is $T_w - T_\infty = Ax^n$, where $A$ is constant. For such a power law variation on wall temperature or mass concentration, the similarity formulation holds good.[19,20] The results are presented for a range of Prandtl number from 0.01 to 1000 and $n>0$. In the formulation it is assumed that the plate thickness is negligibly small compared with its length, hence the conduction within the body of the plate is neglected. In the case of the plate being heated from the ambient fluid, the surface temperature can be well represented by the power law variation from the leading edge, assuming constant surface heat transfer coefficient. The present results are also useful for the case of mass transfer to the plate such as in electroplating.[17] Flows with large Prandtl number may result in chemical processing of hydrocarbons and silicone polymers.[21] Also, large Schmidt number is encountered in mass transfer case. Hence, asymptotic steady state solutions at large Prandtl number are also presented.

## Transient solution

The momentum and energy equations governing the heat transfer from a continuously moving plate whose variable surface temperature undergoes step change with time are similar to those equations given by Gorla[19] in case of transient mass transfer to a continuous moving sheet electrode. These equations in nondimensional form after similarity transformation are given as

$$f''' + \frac{ff''}{2} = 0 \tag{1}$$

$$Pr(1 - f'\tau)\frac{\partial\theta}{\partial\tau} = \frac{\partial^2\theta}{\partial\eta^2} + \frac{Prf}{2}\frac{\partial\theta}{\partial\eta} - nPrf'\theta \tag{2}$$

The initial condition is $\theta(\eta, 0)=0$ and the boundary conditions are $f(0)=0$, $f'(0)=1$, $f'(\infty)=0$, $\theta(0,\tau)=1(\tau)$ and $\theta(\infty,\tau)=0$. Here the prime denotes the differentiation with respect to $\eta$. The solutions for the velocity profiles are known.[4] The energy

Address reprint requests to Dr. Revankar at the Department of Nuclear Engineering, Purdue University, West Lafayette, IN 47907, USA.

Received 13 September 1988; accepted 16 June 1989

© 1989 Butterworth Publishers